Journal of Polymers and the Environment
https://doi.org/10.1007/s10924-025-03515-6

ORIGINAL PAPER

Utilization of Bio-based Monomer Derived from Camelina Oil and Itaconic Acid for the Synthesis of Film-forming Latexes

Martin Kolář[1] · Jan Honzíček[1] · Štěpán Podzimek[1,2] · Martin Hájek[3] · Vladimír Lukeš[4] · Erik Klein[4] · David Kocián[3] · Jana Machotová[1]

Accepted: 24 January 2025

Abstract

The need for the production of synthetic polymers from renewable and sustainable resources also affects the area of emulsion polymerization. The bio-based monomer (BBM) was synthesized from camelina oil (CO) and itaconic acid through transesterification and epoxidation of CO, followed by itaconation, resulting in a blend of methyl esters of CO-originated fatty acids functionalized with reactive methyl itaconate groups. Various amounts of BBM (0−30 wt% of BBM in the total monomer mixture) were copolymerized with standard petroleum-based acrylic monomers (specifically methyl methacrylate, butyl acrylate, and methacrylic acid) using the emulsion polymerization technique to obtain film-forming latexes. Infrared and Raman spectroscopies evidenced the successful incorporation of BBM into the structure of latex polymers. The ultra-high molar mass nanogel fraction was detected by asymmetric flow-field flow fractionation coupled with a multi-angle light scattering (AF4-MALS) for the BBM comprising copolymers; the higher the BBM content, the more extensive the nanogel fraction. Cross-linking of latex polymers induced by BBM testified to the reactivity of itaconated functions in emulsion polymerization and provided additional evidence of the copolymerization ability of BBM. The incorporation of BBM also resulted in pendulum hardness and glass transition temperature enhancement (about 11% and 9 °C, respectively, in the case of 30 wt% of BBM content in contrast to 0 wt% of BBM content in the copolymer). Coatings with excellent transparency and gloss were obtained from all latexes regardless of the BBM content used. Slightly increased water repellency (about 7 ° increased water contact angle value) and significantly improved water whitening resistance of the coatings (about 80% decreased water whitening after 1-day long water exposure) were found for coatings comprising 30 wt% of BBM in the copolymer, where the water whitening phenomenon was highly dependent on the BBM content.

Keywords Latex Coating · Emulsion Polymerization · Bio-based Monomer · Itaconic acid · Camelina oil · Water Resistance

Introduction

Synthetic polymer latexes are advanced polymeric materials, manufactured using emulsion polymerization, a process that involves the free radical polymerization of emulsified monomers, resulting in the formation of polymer latex particles dispersed in an aqueous medium [1–4]. Emulsion polymerization products find extensive applications as protective and decorative coatings, printing inks, adhesives, and paper coatings [5–8]. Different monomers can be utilized in emulsion polymerization; among the most ordinary are various acrylic and methacrylic acid esters [9]. However, these monomers are commercially obtained from petroleum feedstock. The negative environmental impact leads to increased attention to renewable and eco-friendly alternatives

✉ Jana Machotová
jana.machotova@upce.cz

1 Institute of Chemistry and Technology of Macromolecular Materials, Faculty of Chemical Technology, University of Pardubice, Studentská 573, Pardubice 532 10, Czech Republic

2 Synpo, a. s., S. K. Neumanna 1316, Pardubice 532 07, Czech Republic

3 Department of Physical Chemistry, Faculty of Chemical Technology, University of Pardubice, Studentská 573, Pardubice 532 10, Czech Republic

4 Institute of Physical Chemistry and Chemical Physics, Slovak University of Technology in Bratislava, Radlinského 9, Bratislava SK-812 37, Slovakia

Published online: 10 February 2025

[10–15], where plant oils represent the promising feedstock [16–18]. Various plant oils and their derivatives have been used as BBMs in polymeric reactions, including rapeseed [19], linseed [20], soybean [21], sunflower [22], castor [23], and camelina [24] oil. Camelina oil (CO) is produced by cold pressing the oilseed of the cruciferous plant *Camelina sativa* [25]. Camelina does not compete with other crops in the food industry, since it is frequently grown as a non-food oilseed crop. It contains mainly unsaturated fatty acids (80–90%) with a relatively high content of polyunsaturated acids. In short, it can be stated that the most represented are fatty acids with an 18-carbon chain and the ratio between unsaturated acids with one, two, or three double bonds is almost equal [26–29]. In contrast to common plant oils, CO and its derivatives have been rarely utilized as a raw material for polymer production via emulsion polymerization.

Applying plant oil-based monomers in emulsion polymerization remains challenging [30]. The double bonds present in unsaturated fatty acids are not reactive enough to participate in polymerization; instead, they are preferred for functionalization, resulting in the attachment of groups, reactive in free radical polymerization [31]. For example, plant oil derivatives with acryloyl groups, prepared by epoxidation of double bonds [32] and subsequent acrylation of epoxy groups, have emerged as valuable BBMs for emulsion polymerization [33, 34]. Unfortunately, their manufacturing process requires a non-negligible amount of petroleum-based acrylic acid that is not only environmentally unfriendly and flammable but also can cause severe skin burns and respiratory irritation. Furthermore, eye contact is extremely harmful, and long-lasting exposure can trigger allergic reactions [35–38].

Replacement of acrylic acid with itaconic acid in plant oil functionalization is a possible solution to these problems. Itaconic acid is a bio-based chemical manufactured by fermentation of carbohydrates using various fungi, such as *Aspergillus terreus* or *Ustilago maydis* [39–43]. The solid state of itaconic acid also solves the problems arising from the volatility of acrylic acid [44]. Itaconic acid has been utilized in the synthesis of polyesters [45–47], UV-curable coatings [48], and polymeric latexes, although a negative influence on the overall monomer conversion and the copolymerization rate was observed in the emulsion polymerization of acrylic latexes prepared using itaconic acid [49]. Since itaconic acid possesses two carboxylic groups, it cannot be used in the same way as acrylic acid in the case of plant oil functionalization, because the reaction would result in gelation [50]. Utilizing monoesters of itaconic acid is one way to overcome this inconvenience. Several methods of the synthesis of monoesters of itaconic acid have been studied. Báez et al. [51] obtained monomethyl itaconate by esterification of itaconic acid with a large excess of methanol with acetyl chloride used as the initiator. The same synthesis route was also studied by López-Carrasquero et al. [52], who performed the purification step using recrystallization in hot *n*-heptane or *n*-hexane. Richard et al. [53] prepared monoesters of itaconic acid with various alcohols (from C_1 to C_{22}) from itaconic anhydride. Li et al. [54] successfully used monomethyl itaconate for synthesizing itaconated soybean oil which was further used as a replacement for acrylated soybean oil in the synthesis of cross-linked networks. However, the successful utilization of itaconated derivatives of plant oils in emulsion polymerization has not been reported to the best of our knowledge.

The synthesis of partially bio-based compounds manufactured from various plant oils (rapeseed oil, linseed oil, and CO) and petroleum-based acrylic acid and their ability to copolymerize as BBMs with conventional petroleum-based acrylic monomers in standard emulsion polymerization was demonstrated in our previous research [27, 55]. In this work, we present a synthesis of a novel and fully bio-based compound manufactured from CO, a less-explored and non-food oil, and bio-based itaconic acid, specifically, its monomethyl ester (MMI). This paper is also the first report on applying the itaconated CO derivative as a comonomer with conventional petroleum-based acrylic monomers to synthesize film-forming latexes via standard emulsion polymerization technique. The effect of the BBM content on the properties of final latex coating materials was studied, including storage stability, chemical structure, glass transition temperature, molar mass, gloss, hardness, and water resistance.

Materials and methods

Chemicals

Camelina oil (CO, The National Agricultural and Food Center, Pstruša, Slovakia) was modified through transesterification and epoxidation procedures that involved the utilization of hydrogen peroxide (30%, technical grade), methanol, potassium hydroxide, potassium carbonate, and formic acid. All chemicals were obtained from Lach-Ner (Czech Republic). Itaconic acid (Acros Organics, Belgium) was modified through esterification using methanol (Lach-Ner, Czech Republic), benzoyl chloride (Acros Organics, Belgium), toluene (Penta Chemicals, Czech Republic), and petroleum ether (Penta Chemicals, Czech Republic). The synthesis of BBM also involved the use of triphenylphosphine (Sigma-Aldrich, Germany), hydroquinone (Lach-Ner, Czech Republic), ethyl acetate (Lach-Ner, Czech Republic), and sodium bicarbonate (Lach-Ner, Czech Republic).

Methyl methacrylate (MMA), butyl acrylate (BA), and methacrylic acid (MAA) were used as conventional monomers in all emulsion polymerization reactions (Sigma-Aldrich, Germany). Disponil FES 993 (sodium salt of fatty alcohol polyglycerol ether sulphate, BASF, Germany) was used as the surfactant. Ammonium persulphate (Lach-Ner, Czech Republic) served as the initiator, and 2-amino-2-methylpropan-1-ol (AMP 95, Sigma-Aldrich, Germany) was used as the neutralizing agent. All chemicals were used as received without additional purification.

Synthesis and Characterization of Bio-Based Monomer

A multi-step process was employed to obtain the final BBM. Initially, CO transesterification was performed according to references [55, 56] to yield a blend of methyl esters of fatty acids (ME). The detailed proportion of methyl esters of CO-derived fatty acids in the ME intermediate product is given in the reference [27]. In the next step, the double bonds in ME were epoxidized to obtain a blend of epoxidized methyl esters of fatty acids (EME). Furthermore, monomethyl itaconate (MMI) was prepared according to the procedure described in reference [54]. Finally, a blend of methyl esters of fatty acids functionalized with reactive methyl itaconate groups (BBM) was synthesized from EME using a reaction of the epoxy group with MMI following the reference [54]. A detailed procedure of the BBM synthesis pathway is presented in Supplementary Material.

The synthesized BBM and its intermediate products were characterized by the iodine value, epoxy index (EI), proton nuclear magnetic resonance (^{1}H NMR) spectroscopy, infrared (IR) vibration spectroscopy, and Raman spectroscopy. The iodine value was measured according to a Hanus method (EN ISO 3961) [57] using a Mettler Toledo T50 Excellence Titrator (Mettler Toledo, USA). The epoxy value was determined according to the CSN EN ISO 3001 standard. ^{1}H NMR spectra were obtained from a Bruker 500 Avance spectrometer (Bruker, Billerica, MA, USA) at 300 K. The samples (50 µl) were dissolved in $CDCl_3$ (1 ml). Spectra were referenced internally to residual $CDCl_3$ and reported relative to Me_4Si ($\delta = 0$ ppm). The intensity of the bands is referenced to the methyl ester group (3 H). IR spectra were recorded on a Nicolet iS50 FTIR spectrometer (Thermo Fisher Scientific, Waltham, MA, USA) equipped with a build-in diamond ATR (attenuated total reflection) crystal in the region of 4000–400 cm^{-1} (data spacing = 0.5 cm^{-1}). Raman spectra were obtained from the same spectrometer using the FT-Raman module (Nd: YAG excitation laser, $\lambda = 1064$ nm, power = 0.5 W, data spacing = 2 cm^{-1}) in the region of 4000–200 cm^{-1}.

Thermodynamic Calculations of Itaconation Reaction

Theoretical calculations of the itaconation reaction were performed using the Gaussian 16 program package [58]. The optimal geometries of the reactants (epoxidized methyl esters of fatty acids and MMI) and the products (itaconated methyl esters of fatty acids) were optimized using a hybrid M06–2X functional without any constraints (energy cutoff: 10 − 5 kJ/mol: final RMS energy gradient < 0.01 kJ/mol/Å). The M06–2X functional is a reliable approach to determining the thermochemistry of organic compounds [59]. Applying a sufficiently large 6–311 + + G (d, p) basis set [60, 61] including diffuse and polarization functions, allows a balanced description of all investigated species.

Synthesis and Characterization of Latexes

Various amounts of BBM were copolymerized with standard petroleum-based acrylic monomers (0−30 wt% of BBM in the total monomer mixture) using semicontinuous non-seeded emulsion polymerization [55]. The monomer composition of the latex samples is described in Table 1. The monomer composition of all synthesized latexes maintained a constant MMA/BA ratio of 21/28 (w/w) to ensure film-formation of latex films at common ambient temperatures (using the Fox equation [62], the glass transition temperature (T_g) was calculated to be approximately 0 °C for the MMA/BA/MAA (42/56/2 by weight) reference copolymer)

Table 1 Monomer composition of the reference latex (REF) and BBM-comprising latexes (L)

Sample	Monomer (wt%)			
	BBM	MMA	BA	MAA
REF	0	42	56	2
L_5	5	39.8	53.2	2
L_10	10	37.8	50.2	2
L_15	15	35.6	47.4	2
L_20	20	33.4	44.6	2
L_25	25	31.4	41.6	2
L_30	30	29.2	38.8	2

and also to show the effect of the BBM content in a standard film-forming acrylic composition on coating properties, including hardness and T_g. In all monomer compositions, a constant amount (2 wt%) of MAA was introduced to ensure the colloidal stability of latexes through carboxyl functionalities. A detailed procedure of the latex synthesis is presented in Supplementary Material. Each latex sample was prepared three times to determine reproducibility. The coagulum content, solid content, and fractional conversion related only to petroleum-based acrylic monomers (total monomer conversion was not determined due to the high boiling point of BBM occurring in the polymer decomposition region) were determined using standard methods [63] that are presented in more detail in Supplementary Material. The latexes were alkalized to pH 8.5 by 50% AMP 95 aqueous solution. The targeted solid content of final latexes was approximately 39 wt%.

The apparent viscosity of the latexes was assessed at 25 °C using a Brookfield LVDV-E Viscometer (Brookfield Engineering Laboratories, USA) at 100 rpm according to CSN ISO 2555. The storage stability of the final latex copolymers was evaluated according to changes in their particle size and zeta potential after storage for 3 months at elevated temperature (40 °C). The average particle size (hydrodynamic diameter) and zeta potential of the latex particles dispersed in water were detected at 25 ° C by dynamic light scattering (DLS) using the Litesizer 500 instrument (Anton Paar, Austria). The latexes were diluted to approximately 0.01 wt% before the DLS measurement.

Characterization of Copolymer Structure

The structure of latex copolymers was evaluated in terms of their molar mass, cross-link density, and chemical composition using IR vibration spectroscopy and Raman spectroscopy. The molar mass distribution, molar mass average, and the root mean square (RMS) radius (also called the radius of gyration) were obtained by asymmetric flow field flow fractionation combined with a multiangle light scattering detector (AF4-MALS). The experimental AF4-MALS setup consisted of an Agilent 1260 Infinity II chromatograph (Agilent, Santa Clara, CA, USA) coupled with an A4F system Eclipse, a MALS photometer DAWN, and an Optilab refractive index (RI) detector. A channel of 350 µm thickness with a regenerated cellulose membrane (10 kDa cutoff) was utilized for the separation using tetrahydrofuran (THF) as the carrier. The cross-flow profile was as follows: 2.5 mL·min^{-1} for 5 min, linear gradient to 0.1 mL / min over 15 min, 20 min at 0.1 mL/min, and 10 min with zero cross flow. The channel flow and detector flow were 1 and 0.5 mL/min, respectively. Samples were prepared as THF solutions with an estimated concentration of 2.5 mg/mL. The solutions were filtered with a 0.45 µm filter, and injected in a volume of 100 µL. Data collection and processing were performed using ASTRA 8, while VISION 3 was used to operate the Eclipse instrument. Eclipse, detectors, and software were obtained from Waters Wyatt Technology (Santa Barbara, CA, USA).

For determining the cross-link density and chemical composition of latex copolymers, free-standing films having a thickness of about 0.7 mm were prepared by pouring the latexes into silicone molds. The films were dried at ambient temperature (22 ± 1 °C) for 4 weeks and then vacuum-dried at 27 °C for 1 week. The cross-link density was determined through swelling experiments on dry gel polymer samples submerged in toluene at 40 °C for 14 days. The method using a set of equations [64] based on the Flory and Rehner theory [65] was utilized to calculate the cross-link density, expressed as moles of cross-links per cm^3 of a polymer network. Calculations were performed for the MMA/BA/MAA (42/56/2 by weight) copolymer using density and solubility parameter literature data for poly(MMA), poly(BA), and poly(MAA) homopolymers [66, 67]. Data from the literature for the poly(BBM) homopolymer were absent, therefore, the copolymerized BBM monomer was not considered in the calculations. The cross-link density determination is presented in more detail in Supplementary Material. The chemical composition of latex copolymers was studied by IR vibration spectroscopy and Raman spectroscopy under the same experimental conditions as previously mentioned.

Preparation and Characterization of Latex Coatings

Latexes were cast onto glass and steel panels using a box ruler with an adjustable slot. No coalescing agents or latex paint additives were used. The coatings were left to dry under ambient conditions (22 ± 1 °C, 40 ± 5% of relative humidity) for 10 days. Subsequently, the coatings applied to glass panels (ruler slot of 120 µm, dry film thickness of 45 ± 10 µm) were evaluated for their gloss, transparency, water contact angle (WCA), water whitening, glass transition temperature (T_g), and pendulum hardness. The coatings applied to steel panels (steel class 11-ISO 3574 CR1, ruler slot of 200 µm, dry film thickness of 70 ± 10 µm) were evaluated for their mechanical properties (cupping test, impact test, and bending test). Further, the coating susceptibility to solvent penetration was evaluated by water and toluene uptake measurements.

For the gloss measurement, the coatings were applied using a blade applicator onto a glass panel coated with black matte paint (RAL 9005). Gloss was measured with the micro-TRI-gloss µ instrument (BYK-Gardner, Germany) using a gloss measurement geometry at 60 °. The

WCAs were measured using an optical tensiometer (Dataphysics Instruments, Germany) applying a 10 µl water drop. Ten measurements under ambient conditions were taken for each sample. To objectively assess the transparency and water whitening of coating films applied to glass panels, light transmission was measured at a wavelength of 500 nm (corresponding to cyan light which is sensitive for the human eye) employing a ColorQuest XE spectrometer (Hunterlab, USA). The coatings were submerged in distilled water for 4 and 24 h and the transmittance of the exposed coating film area was recorded. The extent of water whitening W (%) was then calculated using Eq. (1):

$$W = 100 \times \frac{T_0 - T_t}{T_0} \tag{1}$$

where T_0 is the coating transmittance before exposure to water and T_t is the coating transmittance measured immediately after exposure to water.

The T_g of the coating polymers scraped off the glass substrate was measured using the differential scanning calorimetry (DSC) technique on a DSC Q2000 instrument (TA Instruments, USA) at a heating rate of 10 °C/min from −40 to 100 °C. The pendulum hardness of the coatings was evaluated according to CSN EN ISO 1552 using a Persoz-type pendulum TQC SP0500 (TQC Sheen, The Netherlands). The pendulum hardness of coatings was measured by the count of the pendulum oscillations with an electronic counter. First, the oscillation counts of the pendulum on the glass plate (reference) were adjusted to 423 ± 3 when the pendulum's amplitude decreased from 12 to 4°. Then the oscillation counts of the pendulum on coatings with glass plate as the substrate were measured and recorded as n. The relative pendulum hardness H (%) was calculated using Eq. (2):

$$H = 100 \times \frac{n}{423} \tag{2}$$

Mechanical properties of coatings were evaluated according to the following tests: cupping test according to CSN EN ISO 1520 on an Elcometer 1620 cupping tester, bending test according to CSN EN ISO 1519 on an Elcometer 1506 cylindrical mandrel bend tester, and the impact test according to CSN EN ISO 6272-1 on an Elcometer 1615 variable impact tester. All the Elcometer instruments are products of Elcometer Instruments, UK. For water and toluene uptake testing, free-standing films of approximately 0.7 mm thickness (prepared in the manner given above) were used. The solvent uptake by a latex film was determined from swelling experiments on film samples of the approximate dimensions $20 \times 20 \times 0.7$ mm^3 immersed in the respective solvent at ambient temperature for 7 days. At the end of the swelling experiment, the soaked film samples were taken out, carefully blotted with filter paper, and weighed. The solvent uptake (U) was calculated using Eq. (3):

$$U = 100 \times \frac{w_t - w_0}{w_0} \tag{3}$$

where w_0 is the weight of a film sample before immersion in solvent and w_t is the weight of the swollen film sample.

The design and objectives of the presented research are summarized in Fig. 1.

Results and Discussion

Characterization of Bio-Based Monomer

The number of double bonds, calculated from the iodine value, and the number of epoxy groups, expressed as the epoxy value, were determined in ME, EME, and BBM (Table 2). The epoxy groups in EME were evidenced by an epoxy value, and their formation was also confirmed by a drop in the level of unsaturation, although some double bonds were found to be non-epoxidized. After the itaconation of EME, an increased iodine value was determined for BBM, which can be attributed to the presence of methyl itaconate functions in BBM molecules. A theoretical amount of MMI that could be bonded via epoxy groups in 100 g of EME is approximately 46.8 g (calculated based on the determined epoxy value for EME). However, the results of the iodine values for EME and BBM indicate that the real amount of reacted MMI was much lower; approximately 11.1 g of MMI was bonded in 100 g of BBM, which means that only approximately 25% of epoxy groups had been successfully itaconated (the rest of non-itaconated epoxy groups was lost by side reactions, probably with hydroxyl groups obtained as a result of the itaconation reaction, or hydrolysis occurring during BBM purification).

The itaconation of EME was followed by NMR spectroscopy. ^{1}H NMR spectrum of EME (Fig. 2) shows characteristic signals of residual vinylene function at 5.25–5.60 ppm (denoted a), the methyl ester group at 3.62 ppm (denoted b), and the CH group of epoxy cycles in the region 2.8–3.2 ppm (denoted c and d). Upon synthesis of BBM, the high conversion of the epoxy function is evident from the disappearance of the signals c and d. The introduction of methyl itaconate into the BBM structure is proven by the appearance of new signals at 6.34, 5.68, and 3.32 ppm (denoted e, f, and i), assigned to fully esterified itaconic acid. The signal of the methyl itaconate group (signal h) is shifted to a lower field compared to that of the fatty acid methyl esters (signal b) because of the electronic effects of the methylidene

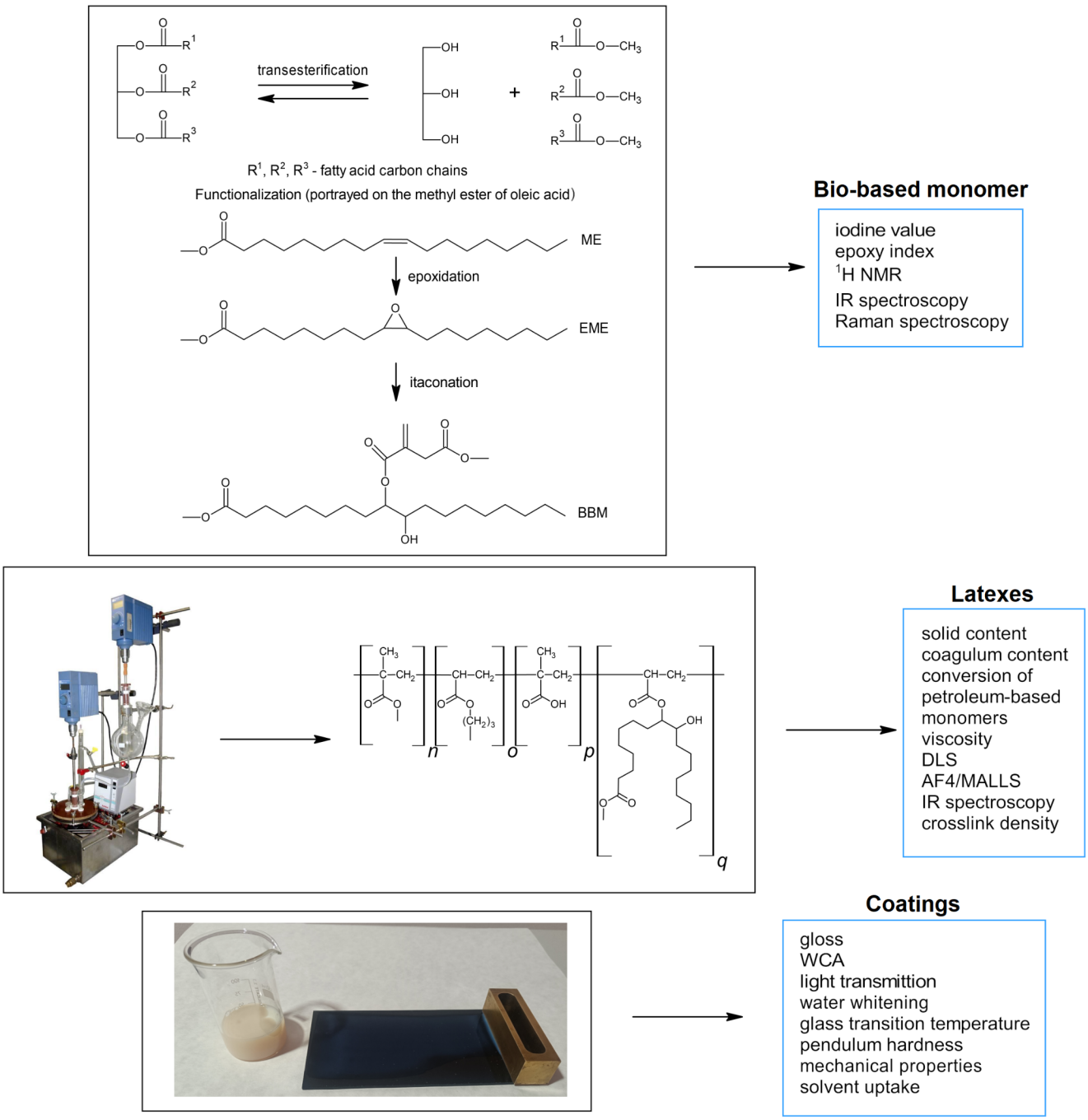

Fig. 1 Schematic design of the synthesis process and overall objectives of the work

Table 2 Iodine and epoxy values of intermediate products and the final BBM

Sample	ME	EME	BBM
Iodine value (g I_2/100 g)	180.2±5.2	32.3±1.2	51.7±2.1
Moles of double bonds/100 g	0.701±0.020	0.127±0.005	0.204±0.008
Epoxy value (moles of epoxy groups/100 g)	0	0.325±0.010	0

function. The signal at 4.88 ppm (signal g) was assigned to the CH group in the fatty acid tail in the α-position relative to the itaconate function. The integral intensities of the signals show that each fatty acid tail in EME contains ~ 0.78 itaconate functions on average. Note that the residues of the starting MMI were detected at 6.41, 5.79, and 3.35 ppm (signals denoted by *), but their content is only ~ 20 mol% (~ 8 wt%).

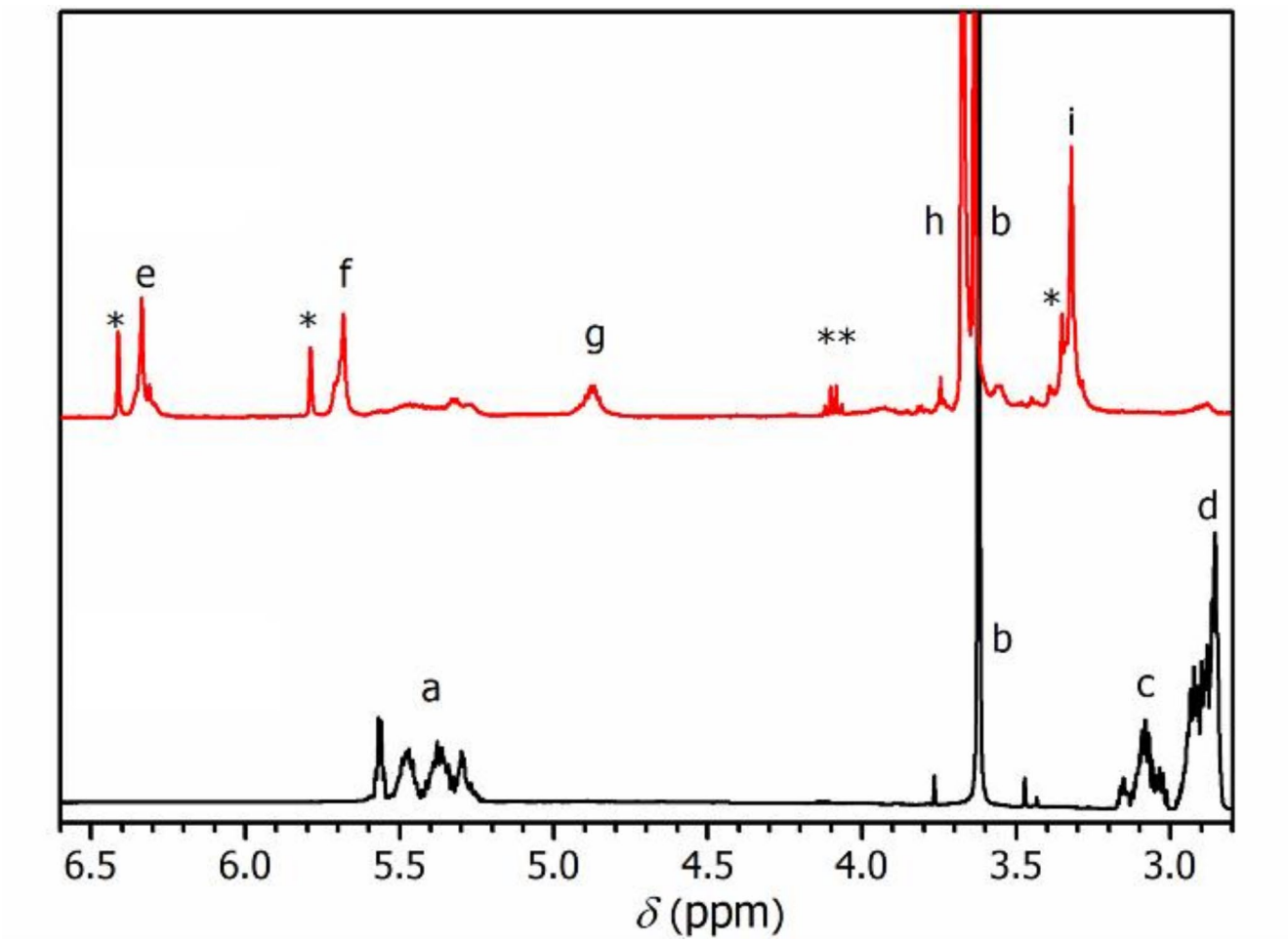

Fig. 2 ^{1}H NMR spectra of EME (black) and BBM (red) with the assignment of characteristic signals. * Residual MMI, ** residual solvents

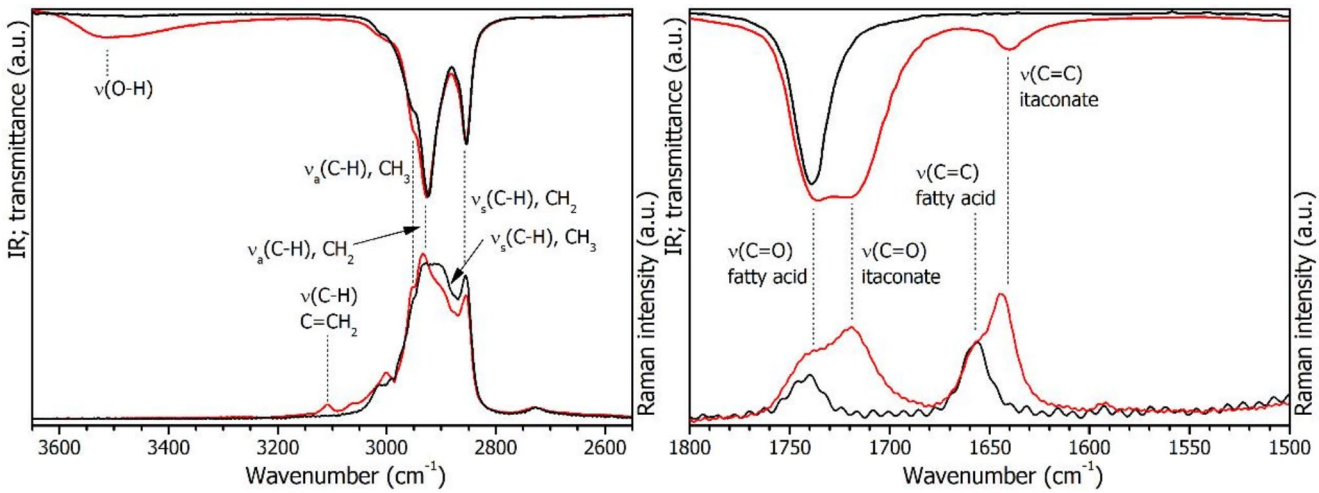

Fig. 3 IR (left) and Raman (right) spectra of EME (black) and BBM (red) with the assignment of characteristic vibration modes

Successful itaconation was further supported by IR and Raman spectra of BBM focusing on the appearance of the characteristic C=C stretching band at 1644 cm^{-1} and the C=O stretching band at 1719 cm^{-1} (Fig. 3). Note that the bands are significantly shifted in comparison to the fatty acid functions as a result of conjugation. The itaconate function also gives the characteristic C–H stretching band of the methylidene group at 3109 cm^{-1}. The formation of hydroxy

function after itaconation is evidenced by the increase in the O–H stretching band at ~3500 cm^{-1} in the IR spectrum.

Composition of Bio-Based Monomer According to Thermodynamic Calculations

The real composition of the synthesized BBM cannot be easily determined due to the formation of many structurally similar compounds (theoretically above 30). The compounds differ in the number of methyl itaconate groups and their position in the fatty acid chain. (In the itaconation reaction step, the epoxy group is transformed into one itaconate and one hydroxyl group). These compounds are almost impossible to separate and identify by common chromatographic methods (standards are not commercially available). Therefore, the thermodynamic calculations of Gibbs energy for the individual itaconation reactions of EME intermediate product with MMI were carried out to estimate the compounds preferred to occur in the BBM final product. The calculations were based on theoretical quantum chemistry (thermodynamic values of the individual reactants and products are not tabulated) implementing the actual reaction conditions (temperature of 293 K and relative permittivity of EME of 6.02). It should be mentioned that the thermodynamic calculations for the particular epoxidation reactions of ME intermediate product were not the subject of this work but were presented in the recent study [68], where low Gibbs energies ranging from −242 to −264 $kJ \cdot mol^{-1}$ were calculated for the individual epoxidation reactions, suggesting their strongly spontaneous character under specified reaction conditions, which has also been evidenced in the reference [69]. (Gibbs energies lower than 0 mean the spontaneous character of a reaction [70]).

The illustrations of the compounds that may be formed in BBM as a result of itaconation of the most represented epoxidized methyl esters of unsaturated fatty acids, namely oleic (C18:1), linoleic (C18:2), and linolenic (C18:3), with calculated Gibbs energy values are presented in Figs. 4–56. As for the double-epoxidized methyl esters of linolenic acid, all the possible reactions were not included because a high number of structurally similar compounds can be formed, requiring time-consuming calculations of Gibbs energies that are not expected to differ significantly. Compounds based on a triple-epoxidized methyl ester of linolenic acid were also not addressed as this intermediate product had not been proven to be formed [71].

In the case of the presented itaconation reactions, Gibbs energy values ranging from −16 to −58 $kJ \cdot mol^{-1}$ were calculated, suggesting that itaconation is less spontaneous compared to epoxidation. The probable reason is the strong exothermic character of epoxidation due to the decomposition of hydrogen peroxide. Focusing on the mono-itaconation reactions, the more spontaneous (i.e., advantageous) position of the methyl itaconate group appears the more distant bonding from the fatty acid head (i.e., the methyl ester group of fatty acid), probably for steric reasons. The calculated Gibbs energies of the mono-itaconation reactions were also found to decrease with the increasing number of double bonds present in the fatty acid tail. This result lets us assume that the presence of double bonds increases the spontaneity of the mono-itaconation reaction. Regarding the double-itaconation reactions, the trends are ambiguous. As for the number of methyl itaconate groups formed, Gibbs energies ranging from −16 to −35 $kJ \cdot mol^{-1}$ were calculated for the mono-itaconation reactions, while Gibbs energies in the range of −37 to −58 $kJ \cdot mol^{-1}$ were obtained for the double-itaconation reactions. These results indicate that the formation of compounds containing two itaconate functions in the final BBM is more spontaneous, i.e., favorable according to the thermodynamic calculations.

Characterization of Latexes

The properties of prepared latexes are presented in Table 3. All synthesized latexes exhibited a low coagulum content which was slightly affected by the amount of copolymerized BBM; the higher the BM concentration in the monomer mixture, the higher the coagulum content formed during

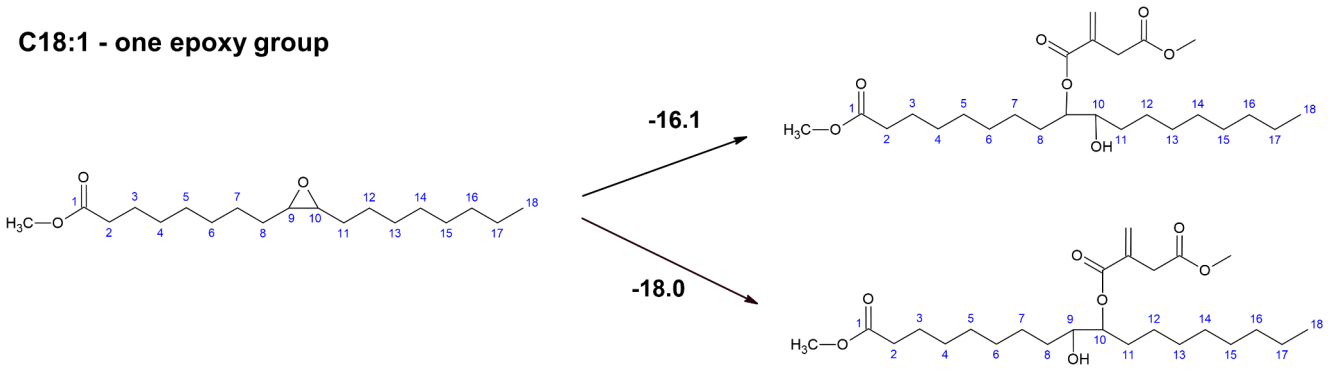

Fig. 4 Compounds that can be formed after itaconation of epoxidized methyl ester of oleic acid with calculated Gibbs energy values ($kJ \cdot mol^{-1}$)

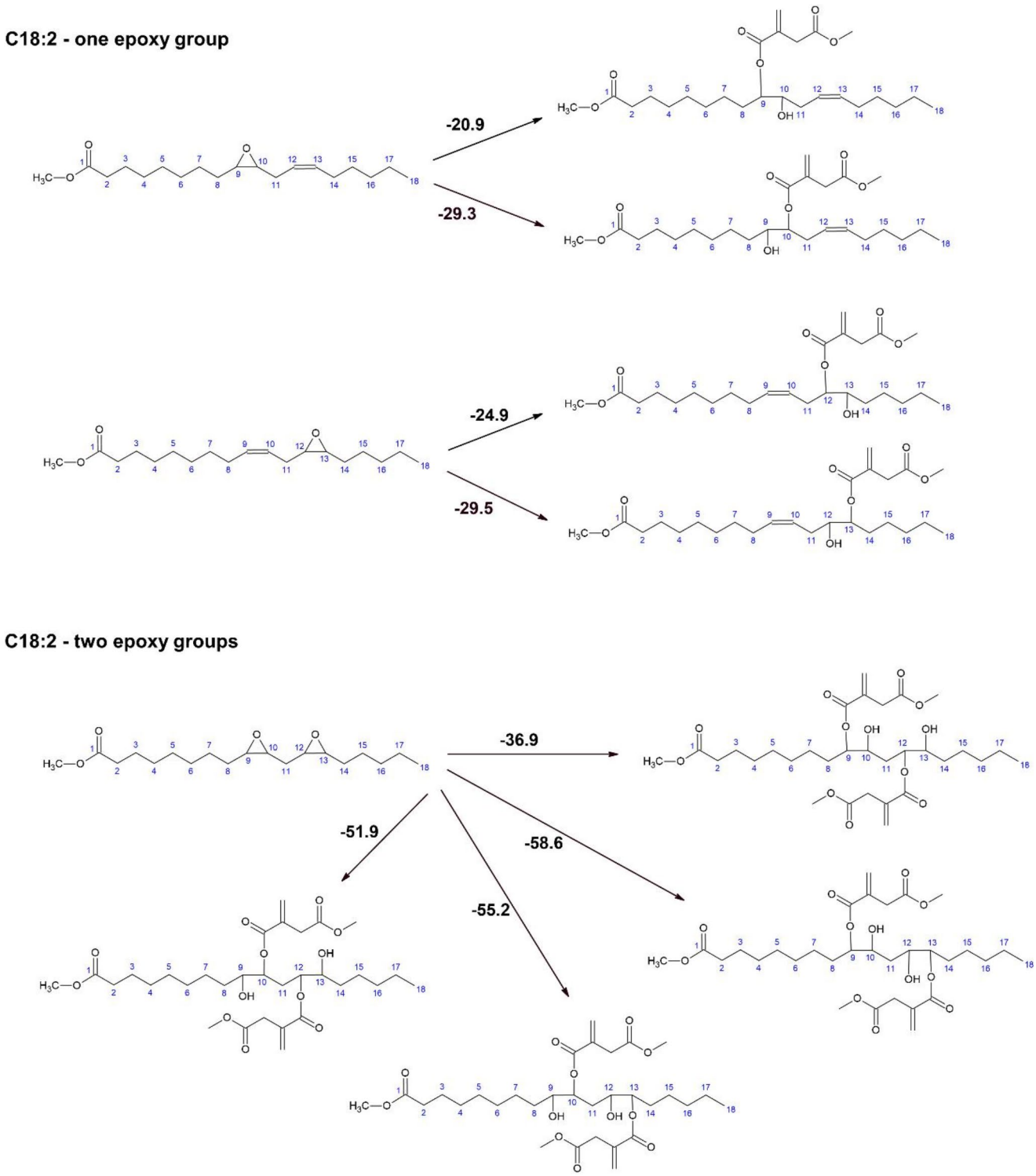

Fig. 5 Compounds that can be formed after itaconation of epoxidized methyl esters of linoleic acid with calculated Gibbs energy values (kJ·mol^{-1})

latex synthesis. The amount of BBM was also shown to have a considerable impact on the conversion of petroleum-based acrylic monomers; a significantly decreased fractional conversion (of acrylic monomers) was found in the case of latexes synthesized using 25 and 30 wt% of BBM in the monomer mixture. This phenomenon has been reported in the relevant literature [30]. It was attributed to BBMs causing a slower polymerization rate and a higher incidence of transfer reactions, probably by trapping propagating macroradicals to give more stabilized species [72]. The decreased

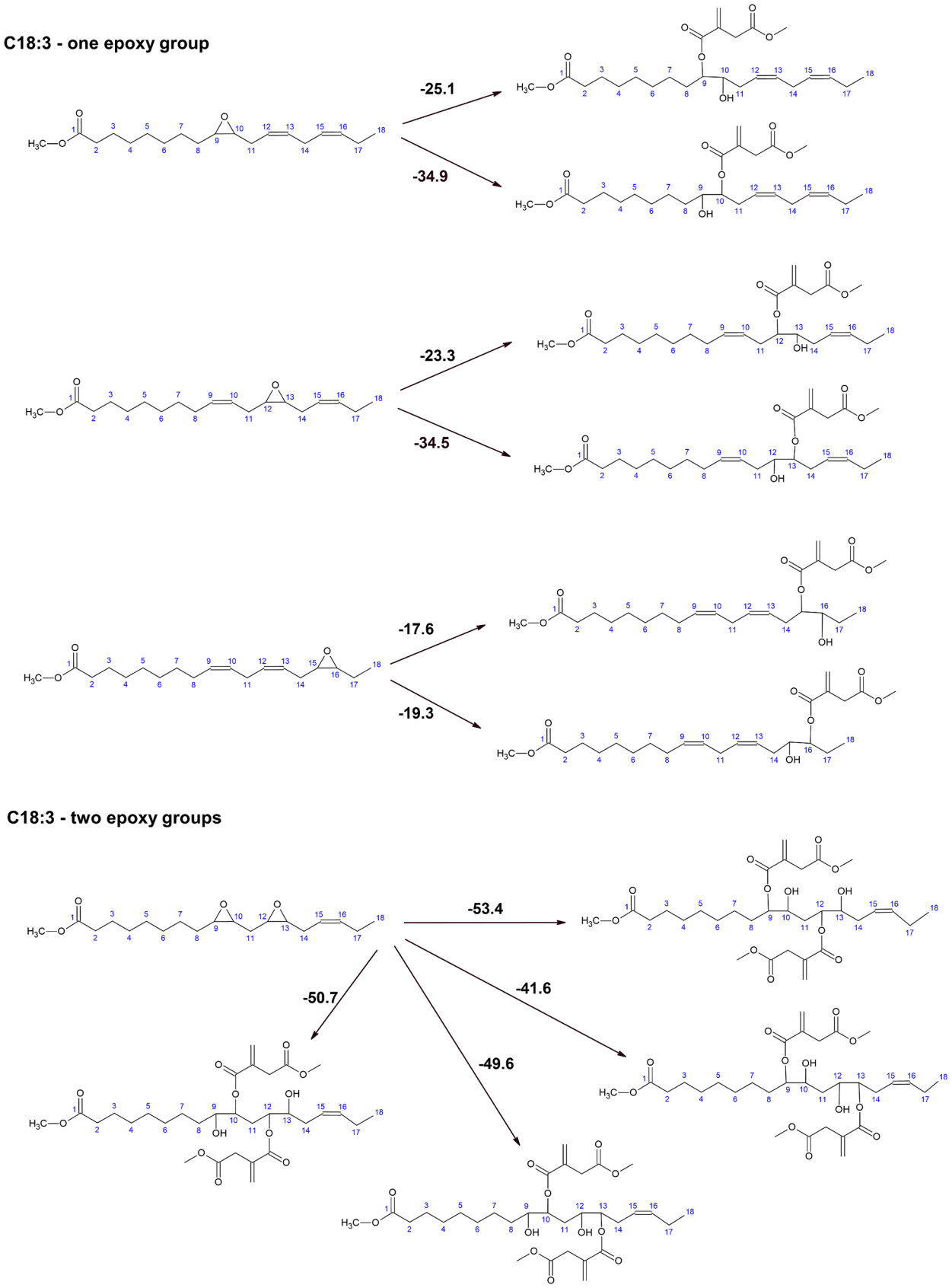

Fig. 6 Compounds that can be formed after itaconation of epoxidized methyl esters of linolenic acid with calculated Gibbs energy values (kJ·mol^{-1})

Table 3 Properties of latexes

Sample	Solid content (%)	Coagulum content (%)	Conversion of petroleum-based monomers (%)	Viscosity	Hydrodynamic diameter (nm)		Zeta potential (mV)	
				(mPa·s)	Initial state	After storage	Initial state	After storage
REF	38.0±0.3	0.7±0.6	94.3±1.0	11.1±0.4	92.1±1.9	94.0±1.6	−42.2±0.2	−38.5±1.1
L_5	37.8±0.2	1.1±0.2	92.9±0.2	18.9±0.3	87.4±2.2	87.0±1.3	−40.1±3.3	−37.3±2.1
L_10	37.9±0.2	0.7±0.1	93.3±0.7	19.5±0.2	85.0±1.1	85.0±1.8	−42.8±0.9	−36.7±1.0
L_15	37.7±0.3	1.2±0.1	91.9±0.5	18.6±0.2	84.8±1.5	85.8±1.4	−48.1±0.3	−41.7±0.6
L_20	36.9±0.2	1.3±0.1	89.1±1.4	19.2±0.3	83.8±0.8	84.3±1.4	−49.4±1.1	−42.9±0.8
L_25	36.0±0.2	1.7±0.2	85.6±1.6	19.8±0.1	80.7±1.6	80.0±1.6	−48.9±2.4	−43.6±0.1
L_30	34.0±0.4	2.6±0.1	76.7±0.6	19.3±0.2	87.0±0.9	87.5±0.9	−51.5±2.3	−43.8±0.5

Table 4 Results of the AF4-MALS analysis (the results are averages from three measurements with the measurement uncertainty below 10%) and cross-link density determined through swelling experiments

Sample	Soluble polymer			Nanogel		RMS radius (nm)	Cross-link density × 10^{-6} (moles of cross-links·cm^{-3})
	M_w (10^3 g·mol^{-1})	Đ	Fraction (%)	M_w (10^6 g·mol^{-1})	Fraction (%)		
REF	6000	36.0	≅100	-[b]	-[b]	120	-[c]
L_5	4300	56.1	41.7	82	58.3	109	3.51±0.2
L_10	6190	12.2	20.7	89	79.3	79	7.59±0.1
L_15	339	20.4	19.1	88	80.9	71	12.6±0.4
L_20	349	15.2	19.3	114	80.7	68	18.8±0.6
L_25	-[a]	-[a]	22.0	81	78.0	60	34.5±1.1
L_30	-[a]	-[a]	14.4	133	85.6	59	61.2±2.9

a Value was impossible to determine due to a low signal of the MALS detector.b The nanogel fraction was not present.c Impossible to determine

conversion of standard acrylic monomers and deteriorated colloidal stability during latex synthesis were also the cause of why no further attempts were made to incorporate a higher BBM content into the latex copolymer.

Further tests revealed that neither the viscosity nor the particle diameter of freshly prepared latexes were influenced pronouncedly by the amount of introduced BBM and can be considered to be driven by the mechanisms of emulsion polymerization [1]. On the contrary, the zeta potential of the freshly prepared latexes (being inherently negative because of the presence of carboxyl and sulphate functions originating from copolymerized MAA, persulphate initiator, and adsorbed anionic surfactant) was found (meant in absolute value) to be proportional to the amount of introduced BBM. This phenomenon can be attributed to partial hydrolysis of the methyl ester functions [73] in the BBM molecules under acidic environment (pH ∼ 2) of emulsion polymerization, which caused the formation of additional carboxyl groups. The zeta potential values (in absolute terms) above −40 mV indicate that all the freshly prepared latexes exhibited colloidal stability [74]. After storage at 40 °C for 3 months, neither visible coagulation nor a significant increase in the average hydrodynamic diameter of the particles were observed. However, a mild reduction in the zeta potential (the absolute value) was found, which can predicate the desorption of some emulsifiers from latex particles [75]. Despite this fact, all latexes can still be considered long-term stable.

Characterization of Copolymer Structure

The weight-average molar mass (M_w), dispersity ($Đ$), z-average RMS radius, and the polymer and nanogel fractions are summarized in Table 4. Similarly to our previous research on latex copolymers synthesized from acrylated BBMs [27], the RI fractograms show two peaks (an example is shown in Fig. 7). (The RI fractogram is a signal of RI detector which is directly proportional to the concentration of molecules eluting from the separation channel). The baseline-separated two peaks indicate fractions with completely different molecular sizes. The peak at lower retention times can be assigned to dissolved individual macromolecules, while that at higher retention times corresponds to swollen cross-linked latex particles (nanogels). As expected, with increasing BBM content, nanogels become more compact, which is evident from the decreasing retention time and RMS radius, as shown in Fig. 8. Figure 8 also reveals a slightly decreasing RMS radius with increasing retention time. This tendency was found for all the tested samples. Decreasing the RMS radius while concurrently increasing retention time, i.e., increasing hydrodynamic volume, may suggest that the central parts of nanogels became more compact. To the authors´ knowledge, such behavior has not been reported in

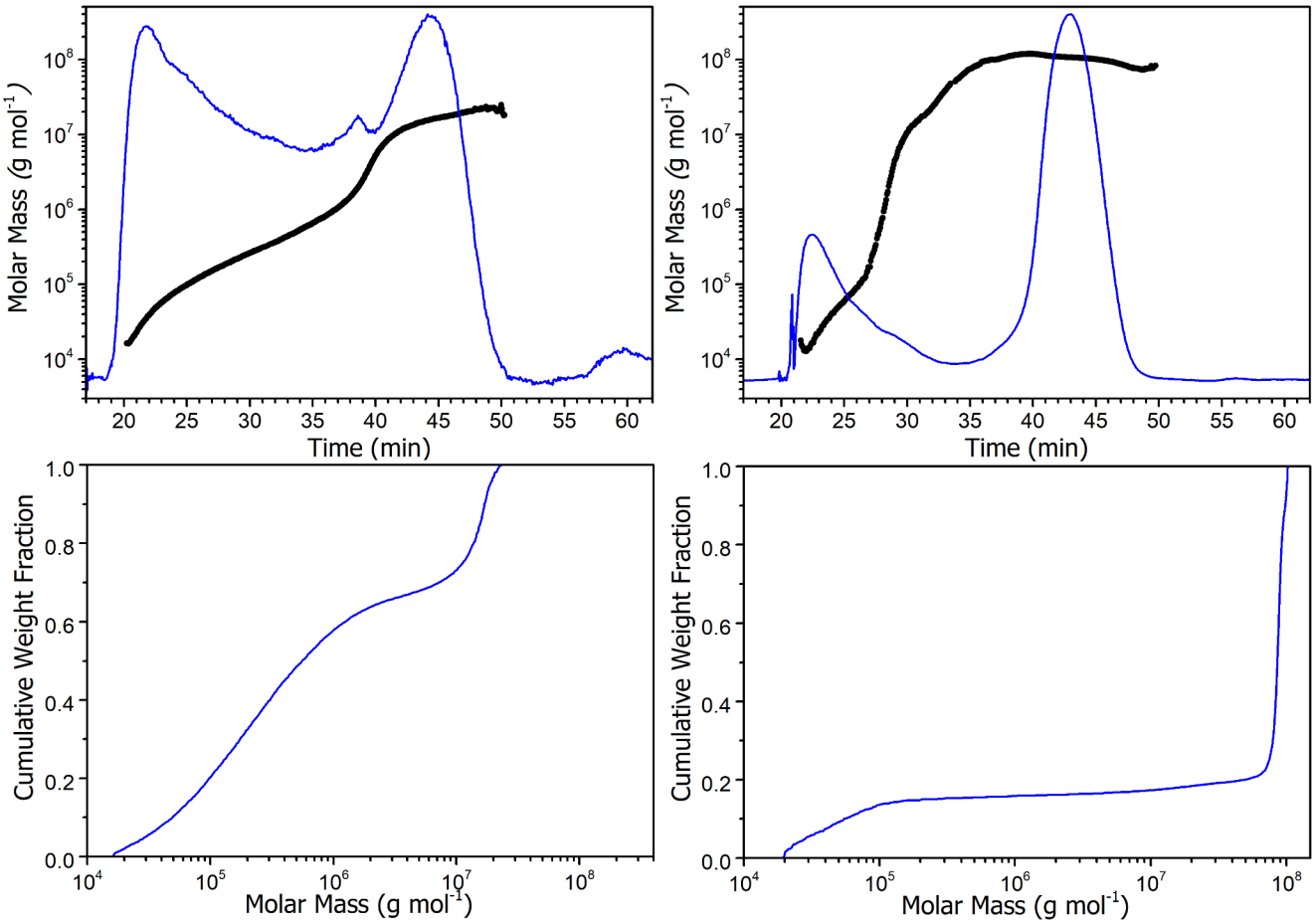

Fig. 7 Molar mass versus retention time plot (black) overlaid with RI fractogram (blue) and cumulative molar mass distribution curves of latex copolymers: REF (left), L_10 (right)

the literature dealing with the characterization of emulsion nanogels but has been observed for topological polymers [76, 77]. The hypothesis is based on the general separation mechanism of AF4 where the retention time increases with increasing hydrodynamic volume. Since the hydrodynamic radius and RMS radius are of different definitions, the former representing particle hydrodynamic size, the latter describing the distribution of mass around the center of gravity, one can imagine that the nanogels having different cross-link densities from the center towards the outer layers behave exactly as shown in Fig. 8.

The level of cross-linking incorporated into latex polymers was assessed, considering the nanogel content obtained from A4F and the cross-link density obtained through swelling experiments (Table 4). As expected, the nanogel content and cross-link density were related to the amount of introduced BBM. This effect is a consequence of the copolymerization of multi-itaconated BM fractions represented mainly by linoleic and linolenic fatty acids, which has already been documented in our previous work on latex copolymers with acrylated BBM counterparts [27].

IR spectroscopy was employed to follow the incorporation of BBM into latex polymer chains (Fig. 9). For this purpose, a protocol previously described for acrylated fatty acid methyl esters was used [55]. The increased content of BBM in the starting monomer mixture resulted in polymers with increased intensity of the absorption bands at 2931 and 2855 cm^{-1} assigned to the antisymmetric and symmetric C–H stretching modes of the methylene groups, ν_a(C–H, CH_2) and ν_s(C–H, CH_2), respectively. Thus, the occurrence of methylene groups forming the fatty acid tails could be evidence of successful BBM copolymerization. A similar effect was observed in the Raman spectra (Fig. 9), where the increased amount of incorporated BBM well correlated with the increased intensity of the symmetric CH stretching band of the methylene groups, ν_s(C–H, CH_2), at 2854 cm^{-1}.

Evaluation of Coatings

The coating properties of the latex films are presented in Table 5. All coating samples appeared smooth, glossy, and transparent (see Supplementary Material, Fig. S1), with

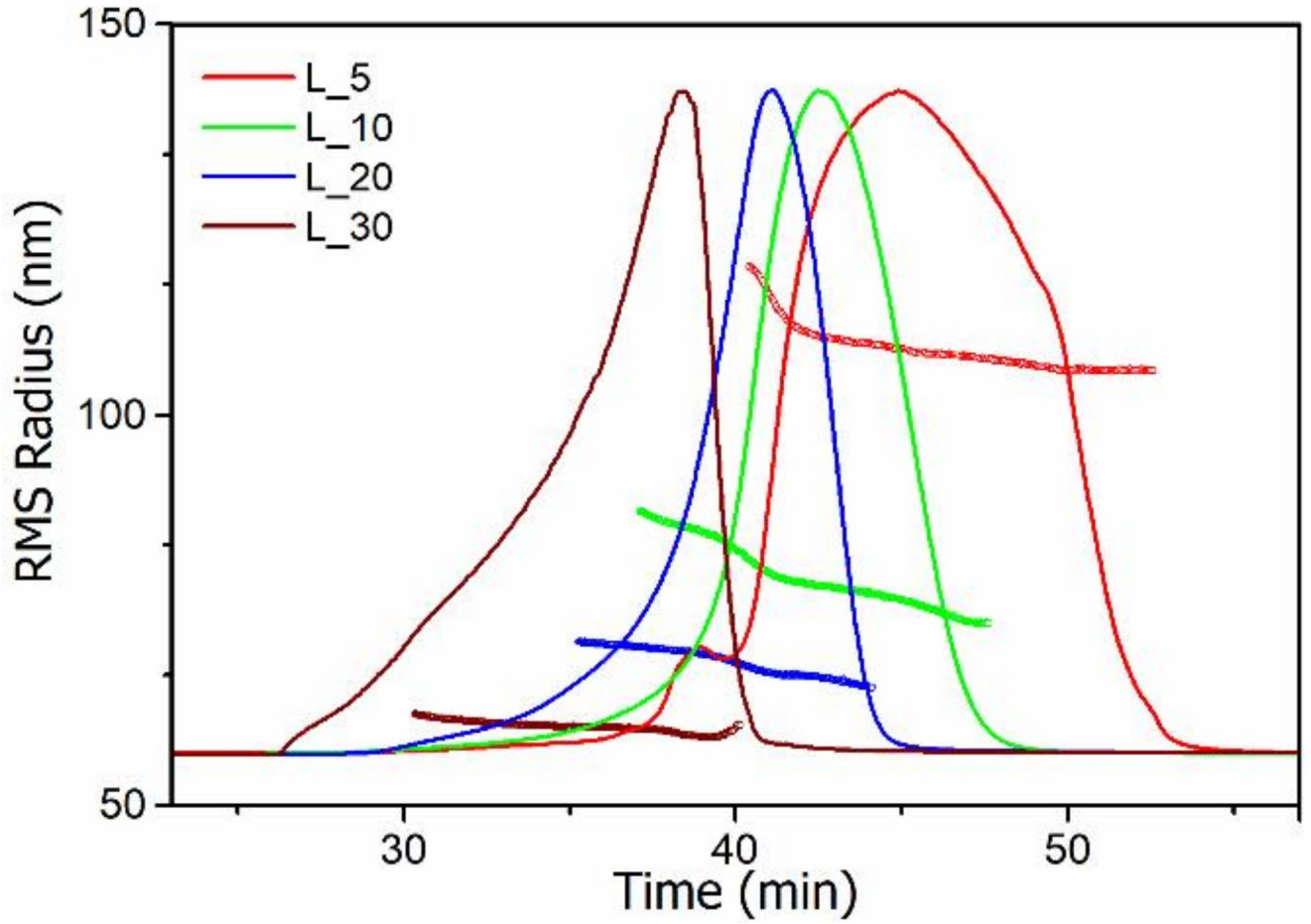

Fig. 8 RMS radius versus retention time plots and MALS fractograms of representative latex copolymers with different amounts of copolymerized BBM

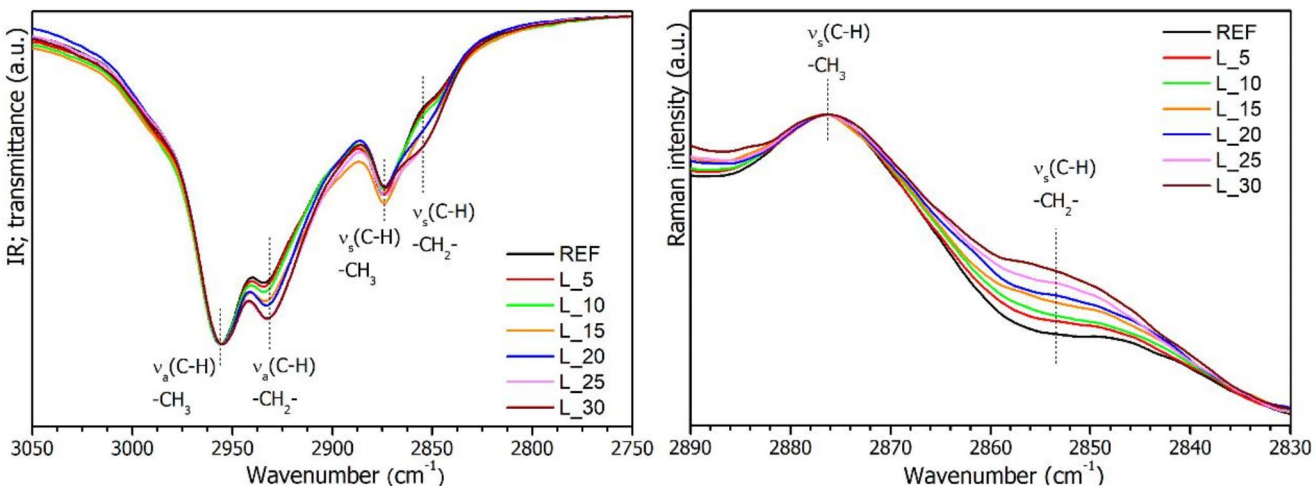

Fig. 9 IR (left) and Raman (right) spectra of latex copolymers with different amounts of copolymerized BBM

gloss and transmittance values comparable to the REF latex coating. It was found that copolymerized BBM decreased coating wettability; almost all BBM-comprising coating samples exhibited about 7 ° higher WCA than REF coating. This phenomenon could be attributed to the hydrophobic nature of the long fatty acid chains in the BBM structure. However, the presence of hydrophilic hydroxyl groups formed as a result of the ring-opening reaction of the epoxy

Table 5 Coating properties of latex films

Sample	Gloss at 60° (GU)	Transmittance at 500 nm (%)	WCA (°)	T_g (°C)	Relative pendulum hardness (%)
REF	83.5±0.1	91.4±0.3	64.9±1.5	1.3±0.3	5.8±0.2
L_5	84.6±0.1	91.2±0.5	70.6±3.5	8.4±0.4	8.4±0.3
L_10	84.5±0.2	90.5±0.4	72.7±2.7	9.3±0.2	8.8±0.6
L_15	83.8±0.1	90.0±0.2	72.5±1.9	10.2±0.3	10.3±0.5
L_20	84.6±0.1	90.3±0.7	72.6±3.7	11.9±0.3	12.3±0.9
L_25	84.2±0.5	90.2±0.5	72.3±0.7	11.1±0.6	10.6±0.6
L_30	84.1±0.1	90.3±0.3	72.6±0.9	12.8±0.2	14.8±1.1

a Impossible to determine

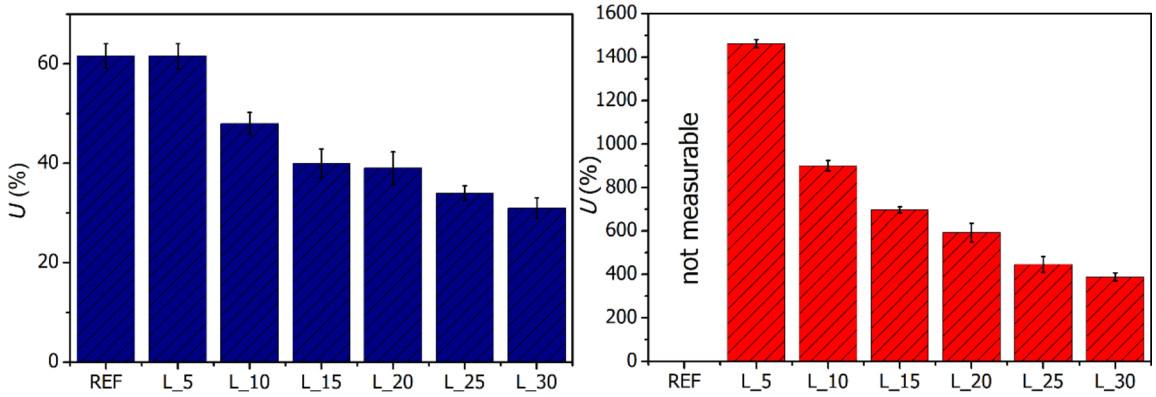

Fig. 10 Water (left) and toluene (right) uptake by the coating films evaluated after 7 days of solvent exposure (toluene uptake by the REF coating film could not be measured due to specimen dissolution)

group (see e.g. Figure 4), probably diminished this effect, leading to similar WCA values regardless of the increasing BBM content.

In our previous research on acrylated BBMs derived from various vegetable oils, including CO [27, 55], a decrease in T_g and pendulum hardness of BBM-comprising coatings was found revealing the plasticizing effect of the fatty acid tails [78, 79] attached to the acrylic polymer backbone. The present study found the opposite effect of the copolymerized itaconated BBM on the T_g and coating pendulum hardness; the higher the BBM concentration, the higher the T_g and pendulum hardness. This phenomenon can be explained by increased cross-link density and the significant contribution of rigid methyl itaconate groups. The latter effect was observed by Li et al. [54] in the case of thermosets based on itaconated soybean oil. These materials had lower cross-link density than those made from acrylated soybean oil but exhibited similar T_g, which was attributed to the higher rigidity of itaconated segments.

Regarding the mechanical properties, all the latex coatings exhibited maximum evaluative values (representing the best mechanical quality determined by the particular test), specifically, > 10 mm for the cupping test, < 4 mm for the bending test, and >100 cm for the impact test. The effect of BBM incorporation on the resistance of coatings against solvent penetration was also tested using solvent (water or toluene) uptake measurements (Fig. 10). The results revealed that the higher the content of the introduced BBM, the lower the solvent uptake by the coating film, suggesting its enhanced barrier protection owing to increased cross-link density.

One of the most pressing shortcomings of common latex protective coating films is their poor water resistance, which manifests itself in the deterioration of protective properties and the appearance of a water-whitening effect. The latter phenomenon is caused by light scattering induced by water clusters formed in the film interior due to water penetration [80]. The results of the water-whitening measurements are presented in Fig. 11 and photographs of films suffering from water-whitening after 24-hour water exposure are presented in Supplementary material (Fig. S1). It was found that the higher the content of the introduced BBM, the lower the water-whitening of the coating films. Moreover, employing high amounts of BBM (25 and 30 wt%) can dramatically improve the resistance of coatings against water whitening, which extends the possibility of their use in various outdoor applications. This phenomenon can be related to the introduced cross-linking that does not allow the water clusters to grow large enough to scatter light visible to the human eye [81].

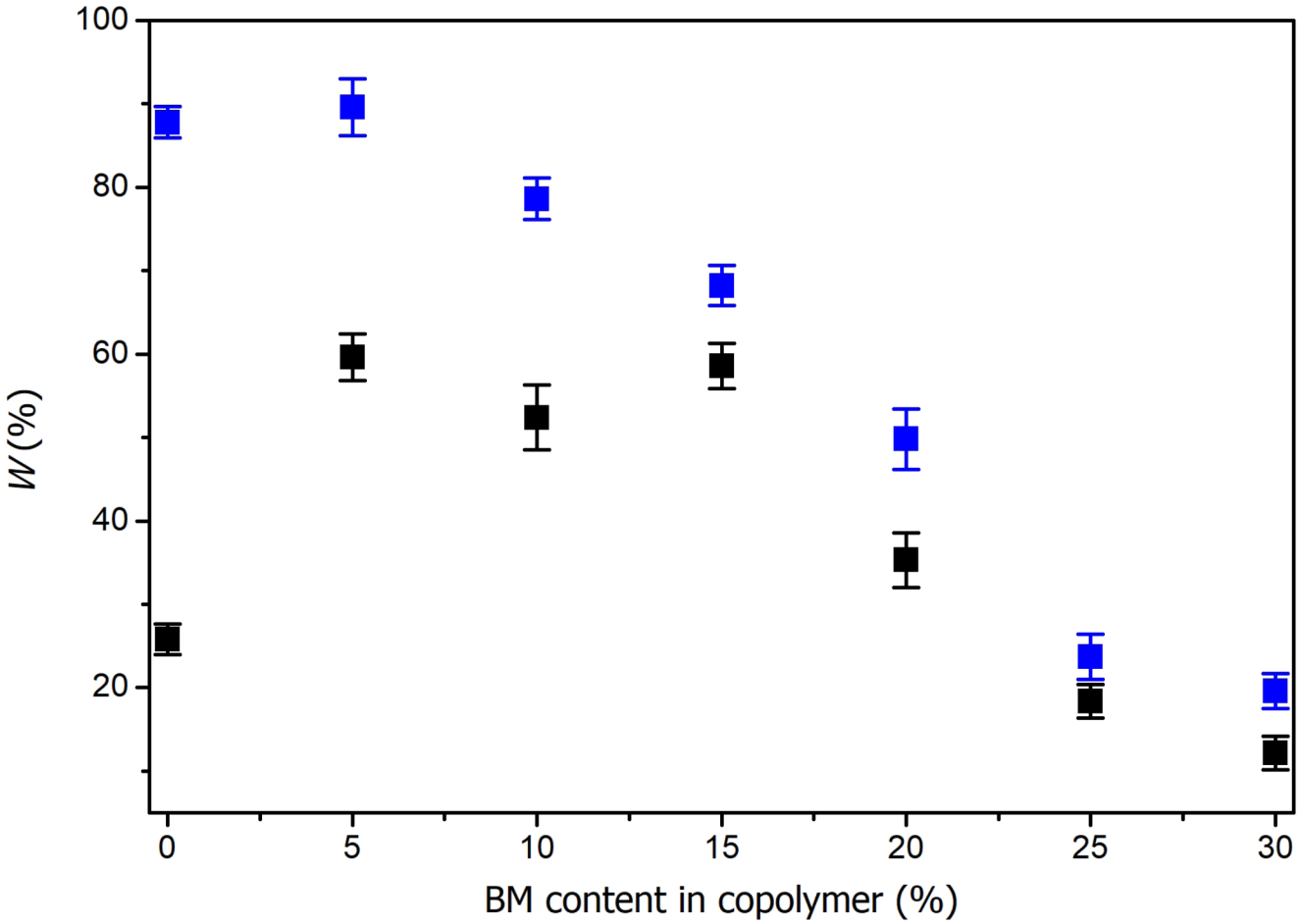

Fig. 11 The degree of water whitening of the coating films evaluated after 4 (black) and 24 (blue) h of water exposure

Conclusion

The bio-based monomer derived from camelina oil and itaconic acid was prepared via a multi-step synthesis consisting of transesterification, epoxidation, and itaconation using monomethyl itaconate. The itaconated derivative of camelina oil was utilized as a reactive comonomer with standard petroleum-based acrylic monomers (0–30 wt% of the bio-based monomer was included in the total monomer mixture) to produce film-forming polymer latexes using a semi-continuous emulsion polymerization technique. Successful polymerizations with conversions exceeding 90% and a coagulum content below 1.5 wt% were performed in the case of compositions containing up to 20 wt% the bio-based monomer in the monomer mixture. A drop in monomer conversion and an increase in coagulum content were observed for the compositions with a higher bio-based monomer content (conversion of 88.8 and 84.5% and coagulum content of 1.7 and 2.6% for the compositions comprising 25 and 30 wt% of the bio-based monomer, respectively). The latex storage stability was not affected by the incorporation and content of the itaconated derivative. Infrared and Raman spectroscopies evidenced the successful incorporation of BBM into the structure of latex polymers. AF4-MALS showed the presence of cross-linked polymers (nanogels) with a molar mass exceeding 10^8 g·mol^{-1}, which is a consequence of the copolymerization of double-itaconated fractions originated mainly from linoleic and linolenic fatty acids. Regarding the coating properties, incorporation of the bio-based monomer did not deteriorate the gloss and transparency of the coating films. The copolymerization of the bio-based monomer caused an increase in T_g and pendulum hardness (about 11 °C and 9%, respectively, comparing the reference and the highest bio-based monomer content coating compositions). This phenomenon indicates the suppression of the long fatty acid tails plasticization by the rigidity of methyl itaconate groups. Utilization of the bio-based monomer significantly enhanced the water-whitening resistance of coating films. These aspects make the itaconated derivative of camelina oil an attractive candidate for replacing standard petroleum-based monomers in producing latex coatings suitable for diverse interior and exterior coating

applications, such as decorative or protective finishes of wooden, metal, and mineral surfaces.

Supplementary Information The online version contains supplementary material available at https://doi.org/10.1007/s10924-025-03515-6.

Acknowledgements We are grateful to the Ministry of Education, Youth and Sports of the Czech Republic, for support through project no. CZ.02.01.01/00/23_021/0008593. This work was also supported by the Slovak Grant Agency (VEGA 1/0461/21).

Author Contributions Conceptualization: J.M.; Methodology: J.H., Š.P., V.L, E.K., and J.M.; Investigation: M.K., J.H., Š.P., and D.K.; Resources: M.K., and J.M.; Data curation: M.K.; Writing—original draft preparation: M.K., J.H., M.H., and J.M.; Writing—review and editing: J.M.; Visualization M.K., J.H., and M.H; Supervision: J.M. All authors have read and agreed to the published version of the manuscript.

Funding Open access publishing supported by the institutions participating in the CzechELib Transformative Agreement.

Data Availability Datasets generated during the study are available at https://doi.org/10.6084/m9.figshare.28219430.

Declarations

Conflict of interest The authors declare that they have no known competing financial interests or personal relationships that could have appeared to influence the work reported in this paper.

Ethical Approval There are no ethical issues involved in this study.

References

1. Thickett SC, Gilbert RG (2007) Emulsion polymerization: state of the art in kinetics and mechanisms. Polymer 48:6965–6991. https://doi.org/10.1016/j.polymer.2007.09.031
2. Lovell PA, Schork FJ (2020) Fundamentals of Emulsion polymerization. Biomacromolecules 21:4396–4441. https://doi.org/10.1021/acs.biomac.0c00769
3. Chern CS (2006) Emulsion polymerization mechanisms and kinetics. Prog Polym Sci 31:443–486. https://doi.org/10.1016/j.progpolymsci.2006.02.001
4. Asua JM (2004) Emulsion polymerization: from fundamental mechanisms to process developments: highlight. J Polym Sci Polym Chem 42:1025–1041. https://doi.org/10.1002/pola.11096
5. Urban D, Takamura K (2002) Polymer dispersions and their industrial applications. Wiley-VCH, Weinheim
6. Asua JM (1997) Polymeric dispersions: principles and applications. Springer Netherlands, Dordrecht
7. Fang C, Zhou F, Zhu X (2021) The application research of benzyl methacrylate (BzMA) in acrylate latex pressure sensitive adhesives. Int J Adhes Adhes 107:102861. https://doi.org/10.1016/j.ijadhadh.2021.102861
8. Ballard N (2024) Designing acrylic latexes for pressure-sensitive adhesives: a review. Polym Int 73:75–87. https://doi.org/10.1002/pi.6596
9. Guerrero-Santos R, Saldívar-Guerra E, Bonilla-Cruz J (2013) Free radical polymerization. In: Saldívar-Guerra E, Vivaldo-Lima E (eds) Handbook of Polymer Synthesis, characterization, and Processing. John Wiley & Sons, Inc., Hoboken, NJ, USA, pp 65–83
10. Alam M, Akram D, Sharmin E et al (2014) Vegetable oil based eco-friendly coating materials: a review article. Arab J Chem 7:469–479. https://doi.org/10.1016/j.arabjc.2013.12.023
11. Gaikwad MS, Gite VV, Mahulikar PP et al (2015) Eco-friendly polyurethane coatings from cottonseed and karanja oil. Prog Org Coat 86:164–172. https://doi.org/10.1016/j.porgcoat.2015.05.014
12. Moreno M, Lampard C, Williams N et al (2015) Eco-paints from bio-based fatty acid derivative latexes. Prog Org Coat 81:101–106. https://doi.org/10.1016/j.porgcoat.2015.01.001
13. Berkak H, Bederina M, Makhloufi Z (2020) Physico-mechanical and microstructural properties of an eco-friendly limestone mortar modified with styrene-polyacrylic latex. J Building Eng 32:101463. https://doi.org/10.1016/j.jobe.2020.101463
14. Onn M, Jalil MJ, Mohd Yusoff NIS et al (2024) A comprehensive review on chemical route to convert waste cooking oils to renewable polymeric materials. Ind Crops Prod 211:118194. https://doi.org/10.1016/j.indcrop.2024.118194
15. Ma Y, Hu Y, Fang Y et al (2024) Recent advances in vegetable oil based fine chemicals and polymers. Green Mater 1–22. https://doi.org/10.1680/jgrma.24.00083
16. Ferreira GR, Braquehais JR, da Silva WN, Machado F (2015) Synthesis of soybean oil-based polymer lattices via emulsion polymerization process. Ind Crops Prod 65:14–20. https://doi.org/10.1016/j.indcrop.2014.11.042
17. Paraskar PM, Prabhudesai MS, Hatkar VM, Kulkarni RD (2021) Vegetable oil based polyurethane coatings– A sustainable approach: a review. Prog Org Coat 156:106267. https://doi.org/10.1016/j.porgcoat.2021.106267
18. Abolins A, Eihe D, Pomilovskis R et al (2023) Rapeseed oil as feedstock for the polymeric materials via Michael addition reaction. Ind Crops Prod 204:117367. https://doi.org/10.1016/j.indcrop.2023.117367
19. Ho YH, Parthiban A, Thian MC et al (2022) Acrylated Biopolymers Derived via Epoxidation and subsequent acrylation of Vegetable oils. Int J Polym Sci 2022:1–12. https://doi.org/10.1155/2022/6210128
20. Ecochard Y, Auvergne R, Boutevin B, Caillol S (2020) Linseed oil-based thermosets by Aza-Michael Polymerization. Eur J Lipid Sci Technol 122:1900145. https://doi.org/10.1002/ejlt.201900145
21. Huang X, Ding Z, Wang W et al (2022) Synthesis and properties of porous materials from polymeric acrylated epoxidized soybean oil via an emulsion template. Ind Crops Prod 188:115662. https://doi.org/10.1016/j.indcrop.2022.115662
22. Asare MA, Kote P, Chaudhary S et al (2022) Sunflower Oil as a renewable resource for polyurethane foams: effects of Flame-Retardants. Polymers 14:5282. https://doi.org/10.3390/polym14235282
23. Laurentino LS, Medeiros AMMS, Machado F et al (2018) Synthesis of a biobased monomer derived from castor oil and

copolymerization in aqueous medium. Chem Eng Res Des 137:213–220. https://doi.org/10.1016/j.cherd.2018.07.014
24. Balanuca B, Raluca S, Hanganu A et al (2015) Design of New Camelina Oil-based hydrophilic monomers for novel polymeric materials. J Am Oil Chemists' Soc 92. https://doi.org/10.1007/s11746-015-2654-z
25. Sydor M, Kurasiak-Popowska D, Stuper-Szablewska K, Rogoziński T (2022) *Camelina sativa*. Status quo and future perspectives. Ind Crops Prod 187:115531. https://doi.org/10.1016/j.indcrop.2022.115531
26. Gesch RW (2014) Influence of genotype and sowing date on camelina growth and yield in the north central U.S. Ind Crops Prod 54:209–215. https://doi.org/10.1016/j.indcrop.2014.01.034
27. Kolář M, Honzíček J, Podzimek Š et al (2023) Derivatives of linseed oil and camelina oil as monomers for emulsion polymerization. J Mater Sci 58:15558–15575. https://doi.org/10.1007/s10853-023-08969-4
28. Arshad M, Mohanty AK, Van Acker R et al (2022) Valorization of camelina oil to biobased materials and biofuels for new industrial uses: a review. RSC Adv 12:27230–27245. https://doi.org/10.1039/D2RA03253H
29. Mondor M, Hernández-Álvarez AJ (2022) Camelina sativa composition, attributes, and applications: a review. Eur J Lipid Sci Technol 124:2100035. https://doi.org/10.1002/ejlt.202100035
30. Demchuk Z, Shevchuk O, Tarnavchyk I et al (2016) Free-radical copolymerization behavior of plant-oil-based vinyl monomers and their feasibility in latex synthesis. ACS Omega 1:1374–1382. https://doi.org/10.1021/acsomega.6b00308
31. Del Rio E, Galià M, Cádiz V et al (2010) Polymerization of epoxidized vegetable oil derivatives: ionic-coordinative polymerization of methylepoxyoleate: Vegetable oil derivatives polymerization. J Polym Sci Polym Chem 48:4995–5008. https://doi.org/10.1002/pola.24297
32. Hattimattur VJ, Sangale VR, Zade PS et al (2018) Review: Epoxidation of Vegetable oils. 5
33. Neves JS, Valadares LF, Machado F (2018) Tailoring acrylated soybean oil-containing terpolymers through Emulsion polymerization. Colloids Interfaces 2. https://doi.org/10.3390/colloids2040046
34. Liu W, Wu M, Ma C et al (2022) Efficient miniemulsion polymerization of Plant Oil-based Acrylate Monomer toward Waterborne Epoxy resins. ACS Sustainable Chem Eng 10:13301–13309. https://doi.org/10.1021/acssuschemeng.2c02403
35. Higgins E, Collins P (2012) Urticarial allergic contact dermatitis caused by UV-cured printing ink. Contact Dermat 66:340–341. https://doi.org/10.1111/j.1600-0536.2012.02010.x
36. Autian J (1975) Structure-toxicity relationships of acrylic monomers. Environ Health Perspect 11:141–152
37. Hideji T, Kazuo H (1982) Structure-toxicity relationship of acrylates and methacrylates. Toxicol Lett 11:125–129. https://doi.org/10.1016/0378-4274(82)90116-3
38. Gelbke H-P, Ellis-Hutchings R, Müllerschön H et al (2018) Toxicological assessment of lower alkyl methacrylate esters by a category approach. Regul Toxicol Pharmacol 92:104–127. https://doi.org/10.1016/j.yrtph.2017.11.013
39. Zhao M, Lu X, Zong H et al (2018) Itaconic acid production in microorganisms. Biotechnol Lett 40:455–464. https://doi.org/10.1007/s10529-017-2500-5
40. Steiger MG, Blumhoff ML, Mattanovich D, Sauer M (2013) Biochemistry of microbial itaconic acid production. Front Microbiol 4. https://doi.org/10.3389/fmicb.2013.00023
41. Devi N, Singh S, Manickam S et al (2022) Itaconic Acid and its applications for Textile, Pharma and Agro-industrial purposes. Sustainability 14:13777. https://doi.org/10.3390/su142113777
42. Becker J, Hosseinpour Tehrani H, Ernst P et al (2021) An optimized Ustilago maydis for Itaconic Acid production at maximal theoretical yield. J Fungi 7:20. https://doi.org/10.3390/jof7010020
43. Geiser E, Przybilla SK, Friedrich A et al (2016) Ustilago maydis produces itaconic acid via the unusual intermediate trans-aconitate. Microb Biotechnol 9:116–126. https://doi.org/10.1111/1751-7915.12329
44. Gnanasekaran R, Saranya P, Yuvashree S et al (2018) Itaconic Acid production by Novel Aspergillus Niveus in Solid State Fermentation using Agrowastes. Int J Eng Technol 7:76–81. https://doi.org/10.14419/ijet.v7i3.34.18777
45. Rubeš D, Vinklárek J, Prokůpek L et al (2023) Styrene-free unsaturated polyester resins derived from itaconic acid curable by cobalt-free accelerators. J Mater Sci 58:6203–6219. https://doi.org/10.1007/s10853-023-08407-5
46. Dai J, Ma S, Wu Y et al (2015) Polyesters derived from itaconic acid for the properties and bio-based content enhancement of soybean oil-based thermosets. Green Chem 17:2383–2392. https://doi.org/10.1039/C4GC02057J
47. Dai J, Ma S, Liu X et al (2015) Synthesis of bio-based unsaturated polyester resins and their application in waterborne UV-curable coatings. Prog Org Coat 78:49–54. https://doi.org/10.1016/j.porgcoat.2014.10.007
48. Brännström S, Malmström E, Johansson M (2017) Biobased UV-curable coatings based on itaconic acid. J Coat Technol Res 14:851–861. https://doi.org/10.1007/s11998-017-9949-y
49. Lock MR, El-Aasser MS, Klein A, Vanderhoff JW (1990) Investigation of the persulfate/itaconic acid interaction and implications for emulsion polymerization. J Appl Polym Sci 39:2129–2140. https://doi.org/10.1002/app.1990.070391008
50. Pérocheau Arnaud S, Andreou E, Pereira Köster LVG, Robert T (2020) Selective synthesis of Monoesters of Itaconic acid with broad substrate scope: Biobased Alternatives to Acrylic Acid? ACS Sustainable Chem Eng 8:1583–1590. https://doi.org/10.1021/acssuschemeng.9b06330
51. Báez ME, Jiménez E, Laredo E et al (2007) Comblike complexes of Poly(itaconic acid) and poly(mono methyl itaconate) and Alkyltrimethylamonium Cationic surfactants. Polym Bull 58:529–539. https://doi.org/10.1007/s00289-006-0688-y
52. López-Carrasquero F, Martinez de Ilarduya A, Cárdenas M et al (2003) New comb-like poly(n-alkyl itaconate)s with crystalizable side chains. Polymer 44:4969–4979. https://doi.org/10.1016/S0032-3861(03)00470-1
53. Richard J-V, Delaite C, Riess G, Schuller A-S (2016) A comparative study of the thermal properties of homologous series of crystallisable n-alkyl maleate and itaconate monoesters. Thermochimica Acta 623:136–143. https://doi.org/10.1016/j.tca.2015.10.015
54. Li P, Ma S, Dai J et al (2017) Itaconic Acid as a Green Alternative to Acrylic Acid for producing a soybean oil-based Thermoset: synthesis and Properties. ACS Sustainable Chem Eng 5:1228–1236. https://doi.org/10.1021/acssuschemeng.6b02654
55. Kolář M, Machotová J, Hájek M et al (2023) Application of Vegetable Oil-based monomers in the synthesis of Acrylic latexes via Emulsion polymerization. Coatings 13:262. https://doi.org/10.3390/coatings13020262
56. Hájek M, Skopal F, Machek J (2008) Simplification of separation of the reaction mixture after transesterification of vegetable oil. Eur J Lipid Sci Technol 110:347–350. https://doi.org/10.1002/ejlt.200700228
57. Yildiz Y, Alfeen M, Yildiz B (2019) Determination of Iodine Value in Triisocetyl Citrate (Citmol-316) by United States Pharmacopeia Hanus Method. Int J Chem Pharm Sci 72:38–41
58. Frisch MJ, Trucks GW, Schlegel HB et al (2016) Gaussian 16 Revision A.03.
59. Zhao Y, Truhlar DG (2008) The M06 suite of density functionals for main group thermochemistry, thermochemical kinetics,

noncovalent interactions, excited states, and transition elements: two new functionals and systematic testing of four M06-class functionals and 12 other functionals. Theor Chem Acc 120:215–241. https://doi.org/10.1007/s00214-007-0310-x
60. Hariharan PC, Pople JA (1973) The influence of polarization functions on molecular orbital hydrogenation energies. Theoret Chim Acta. https://doi.org/10.1007/BF00533485
61. Rassolov VA, Pople JA, Ratner MA, Windus TL (1998) 6-31G* basis set for atoms k through Zn. J Chem Phys 109:1223–1229
62. Fox TG Jr, Flory PJ (1950) Second-order transition temperatures and related properties of Polystyrene. I. Influence of Molecular Weight. J Appl Phys 21:581–591. https://doi.org/10.1063/1.1699711
63. Ling H, Junyan L (2008) Synthesis, modification and characterization of core–shell fluoroacrylate copolymer latexes. J Fluorine Chem 129:590–597. https://doi.org/10.1016/j.jfluchem.2008.04.007
64. Sperling LH (2005) Introduction to physical Polymer Science. Wiley
65. Flory PJ, Rehner J Jr (1943) Statistical mechanics of cross-linked Polymer Networks II. Swelling. J Chem Phys 11:521–526. https://doi.org/10.1063/1.1723792
66. Tobing SD, Klein A (2001) Molecular parameters and their relation to the adhesive performance of acrylic pressure-sensitive adhesives. J Appl Polym Sci 79:2230–2244
67. Vandenburg HJ, Clifford AA, Bartle KD et al (1999) A simple solvent selection method for accelerated solvent extraction of additives from polymers. Analyst 124:1707–1710. https://doi.org/10.1039/A904631C
68. Hájek M, Kocián D, Hájek T et al (2024) Epoxidation of Camelina sativa oil methyl esters as a second-generation biofuel with thermodynamic calculations. Renewable Energy 228:120670
69. Monono EM, Haagenson DM, Wiesenborn DP (2015) Characterizing the epoxidation process conditions of canola oil for reactor scale-up. Ind Crops Prod 67:364–372. https://doi.org/10.1016/j.indcrop.2015.01.061
70. Atkins P, de Paula J, Keeler J (2018) Atkins' Physical Chemistry. Oxford University Press Incorporated, USA
71. Hájek M, Hájek T, Kocián D et al (2023) Epoxidation of Methyl Esters as Valuable Biomolecules: monitoring of reaction. Molecules 28:2819. https://doi.org/10.3390/molecules28062819
72. Vilela C, Rua R, Silvestre AJD, Gandini A (2010) Polymers and copolymers from fatty acid-based monomers. Ind Crops Prod 32:97–104. https://doi.org/10.1016/j.indcrop.2010.03.008
73. Šňupárek J Jr, Tuťálková A (1979) Particle coagulation at semicontinuous emulsion polymerization. II. Characterization of surface groups. J Appl Polym Sci 24:915–921. https://doi.org/10.1002/app.1979.070240404
74. Yilmaz O, Cheaburu CN, Durraccio D et al (2010) Preparation of stable acrylate/montmorillonite nanocomposite latex via in situ batch emulsion polymerization: Effect of clay types. Appl Clay Sci 49:288–297. https://doi.org/10.1016/j.clay.2010.06.007
75. Capek I (2002) Sterically and electrosterically stabilized emulsion polymerization. Kinetics and preparation. Adv Colloid Interface Sci 99:77–162. https://doi.org/10.1016/S0001-8686(02)00005-2
76. Uehara E, Tanaka R, Inoue M et al (2014) Mean-square radius of gyration and hydrodynamic radius for topological polymers evaluated through the quaternionic algorithm. Reactive Funct Polym 80:48–56. https://doi.org/10.1016/j.reactfunctpolym.2014.03.004
77. Uehara E, Deguchi T (2018) Mean-square radius of gyration and the hydrodynamic radius for topological polymers expressed with graphs evaluated by the method of quaternions revisited. Reactive Funct Polym 133:93–102. https://doi.org/10.1016/j.reactfunctpolym.2018.09.007
78. Jia P, Bo C, Hu L, Zhou Y (2015) Synthesis and characterization of glyceryl monooleate-based polyester. Korean J Chem Eng 32:547–551. https://doi.org/10.1007/s11814-014-0214-0
79. Bajetto G, Scutera S, Menotti F et al (2024) Antimicrobial efficacy of a Vegetable Oil Plasticizer in PVC matrices. Polymers 16:1046. https://doi.org/10.3390/polym16081046
80. Khanjani J, Hanifpour A, Pazokifard S, Zohuriaan-Mehr MJ (2020) Waterborne acrylic-styrene/PDMS coatings formulated by different particle sizes of PDMS emulsions for outdoor applications. Prog Org Coat 141:105267. https://doi.org/10.1016/j.porgcoat.2019.105267
81. Machotová J, Kalendová A, Steinerová D et al (2021) Water-resistant latex Coatings: tuning of Properties by Polymerizable surfactant, Covalent Crosslinking and Nanostructured ZnO Additive. Coatings 11. https://doi.org/10.3390/coatings11030347